Eur. Phys. J. B **45**, 219–222 (2005)
DOI: 10.1140/epjb/e2005-00123-6

THE EUROPEAN PHYSICAL JOURNAL B

Partial magnetization reversal using laser annealing in patterned NiFe/FeMn film

S.D. Choi[1], S.W. Kim[1], D.H. Jin[1], M.S. Lee[1], H.W. Joo[1], K.A. Lee[1], S.S. Lee[2], and D.G. Hwang[2,a]

[1] Dankook Univ. Dept. of Physics, Cheonan 330-714, Korea
[2] Sangji Univ., Dept. of Computer and Electronic Physics, Wonju 220-702, Korea

Received 15 September 2004 / Received in final form 10 November 2004
Published online 19 April 2005 –

Abstract. We have studied local magnetization reversal by laser annealing in exchange biased NiFe/FeMn bilayer. Local magnetization reversal was performed by using the Nd:YAG laser under external magnetic field. When the laser illuminated the patterned film with the power of above 300 mW during 15 min, a magnetoresistance (MR) curve with symmetric peaks at the opposite field was obtained due to the local reversal of exchange biasing. A similar result was observed in NiFe/FeMn/NiFe trilayer. As the exposed area expanded, the intensity of opposite MR peak increased. The direction of exchange anisotropy in the partially reversed region can be restored by local laser annealing under alternating magnetic field, even if its MR peak was reduced by the damage and interdiffusion. The magnetic new domain structures of the partially reversed region was generated by laser annealing near the exposed area.

PACS. 75.70.Cn Magnetic properties of interfaces (multilayers, superlattices, heterostructures) – 61.80.Ba Ultraviolet, visible, and infrared radiation effects (including laser radiation)

1 Introduction

The development of alternative logic and non-volatile memory based on ferromagnetic materials has been very active [1–3]. To improve a technical difficulty and simplify the design of the memory device, the current controlled magnetization reversal due to the movement of domain wall and spin transfer in magnetic thin films had been suggested [4,5]. The general method for assigning a magnetic memory device and sensors is to orient the remanent magnetization of small patterned ferromagnetic elements in one of two opposite directions. An external magnetic field and current can control the magnetization reversal of a free ferromagnetic element. However, that of the ferromagnetic elements pinned by antiferromagnet should be realized through thermal process. This way is accompanied with the magnetization of the whole films, and it is hard to get local reversal of magnetization. The locally annealing experiment was performed in ferromagnetic amorphous ribbons by laser [6]. To locally reverse a unidirectional anisotropy in exchange biased films, the laser annealing method was used in this works [7]. In this paper, the partial magnetization reversal of the exchange-biased FeMn/NiFe bilayers and NiFe/FeMn/NiFe trilayer films as a function of intensity, time, and area of the locally exposed laser was investigated.

[a] e-mail: dghwang@sangji.ac.kr

2 Experimental

Multilayer films consisting of Ta(5 nm)/NiFe(11 nm)/FeMn(16 nm)/Ta(5 nm) and Ta(5 nm)/NiFe(11 nm)/FeMn(16 nm)/NiFe(7 nm)/Ta(5 nm) were prepared using ion-beam deposition system. Patterned by the metal shadow mask of 1 mm × 15 mm, the films were exposed to the emission of diode pumped solid state (DPSS, Nd:YAG) laser operating at a wavelength of 532 nm and having a continuous wave (CW) second harmonic generation (SHG) output during 15 min under the applied field of 600 G. The laser beam was focused through an optical fiber into 1 mm circular spot, with the intensity increased up to 440 mW. The direction of applied field ($\boldsymbol{H}_a$) during exposure was opposed to that of the magnetic field ($\boldsymbol{H}_d$) during deposition. The magnetic properties for the exchange biased films were analyzed by the magnetoresistance (MR) curves. The magnetic domain of the exposed region was measured by magnetic force microscope (MFM: Digital Instrument, DI dimension 3100 IVa).

3 Results and discussion

Figure 1 shows the MR curves of the mask-patterned and exchange-biased (a) NiFe(11 nm)/FeMn(16 nm) bilayer and (b) NiFe(11 nm)/FeMn(16 nm)/NiFe(7 nm) trilayer for a various laser power. The MR ratio and the exchange

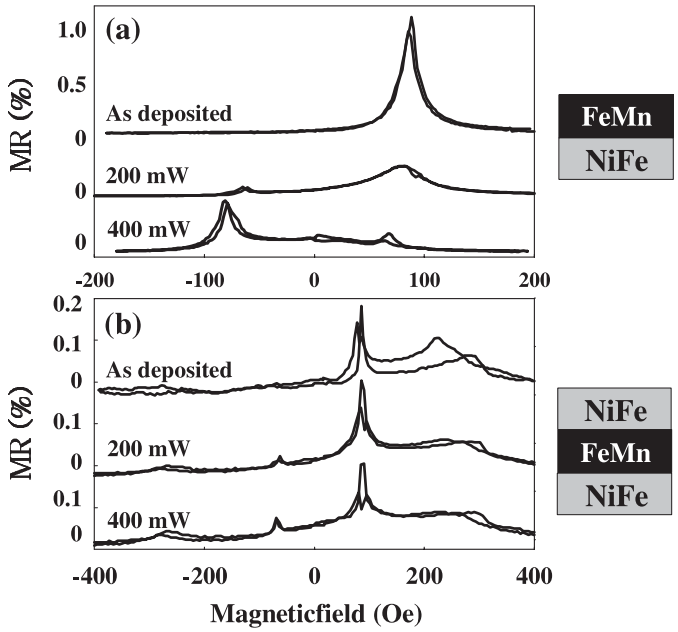

Fig. 1. MR curves as a function of various laser powers in the strip-patterned (a) Ta(5 nm)/ NiFe(11 nm)/FeMn(16 nm)/Ta(5 nm) and (b) Ta(5 nm)/ NiFe(11 nm)/FeMn(16 nm)/NiFe(7 nm)/Ta(5 nm) films.

Table 1. MR ratios and exchange biasing fields ($\boldsymbol{H}_{ex}$) before and after laser annealing.

		as deposited	200 mW	300 mW
Negative MR peak	MR	0.9%	0.2%	0.1%
	$\boldsymbol{H}_{ex}$	+87 Oe	+80 Oe	+76 Oe
Positive MR peak	MR	0%	0.1%	0.3%
	$\boldsymbol{H}_{ex}$	0 Oe	−63 Oe	−80 Oe

biasing field ($\boldsymbol{H}_{ex}$) of as-deposited bilayer were 0.9% and +87 Oe as shown in Table 1, respectively. As the power of laser annealing increase, the intensity of MR peak located in +87 Oe was shrunk. A new MR peak was generated at −63 Oe due to local laser annealing of 200 mW. The location of positive MR peak ($\boldsymbol{H}_{ex}$) of 400 mW changed slightly from +87 to +76 Oe, and MR ratio decreased from 0.9% to 0.1%. On the other hand, the new (negative) MR peak shifted from −63 to −80 Oe, with the ratio increased up to 0.3%. Because the reversal magnetization exposed by the local laser annealing is occurred, the positive peak does not vanish on increasing the laser power, and the rise of negative peak does not lead to amplitude comparable with that of positive peak in the as-deposited sample. The local reversal of exchange anisotropy in the trilayer was similar to the bilayer as shown in Figure 1b. The negative MR peak of exchange-biased NiFe(11 nm) layer was generated at −75 Oe, and its ratio at 400 mW is less than that of bilayer due to the increase of film thickness. The negative MR peak of NiFe(7 nm) layer was also generated at −260 Oe.

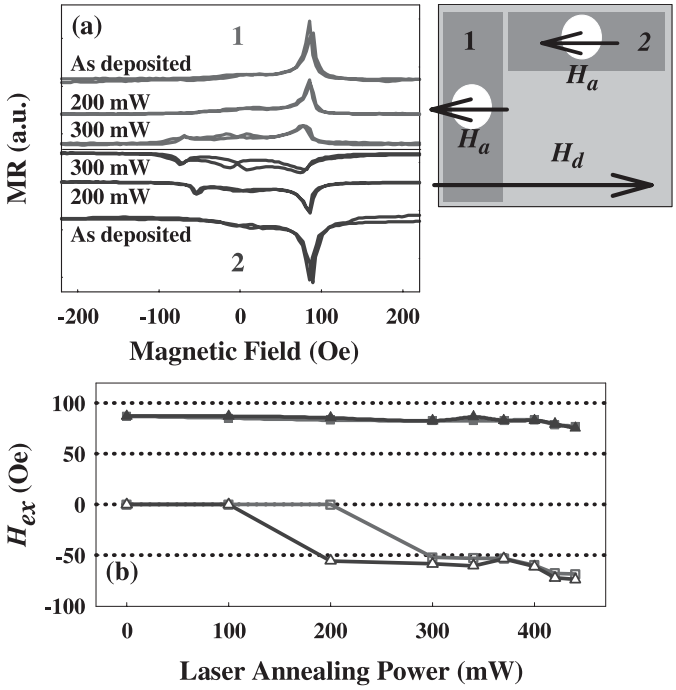

Fig. 2. (a) MR curves of laser annealed samples at as-deposited, 200 mW, and 440 mW annealed films, where 1 is perpendicular and 2 is parallel for an applied magnetic field direction. (b) $\boldsymbol{H}_{ex}$ plotted as a function of laser annealing power, where the direction of strip is perpendicular (square) and is parallel (triangle) for a applied field direction. Here open squares and triangles are the local magnetization reversal $\boldsymbol{H}_{ex}$'s values.

Figure 2 shows the MR curves and the exchange biasing field ($\boldsymbol{H}_{ex}$) of reversed region as a function of laser power in the two bilayers, which were (triangle) parallel and (square) perpendicular between the strip direction and the applied field. The negative MR peak in the parallel sample was generated at 200 mW. On the other hand, the perpendicular one did not reveal at 200 mW, but appear at 300 mW as shown in Figure 2a. This suggests that the domain wall generated by the local magnetization reversal of two samples has a different structure. The conduction electron in the 180 Bloch wall of a head-on-head type (parallel sample) will be more scattered than the normal Bloch wall (perpendicular one).

Figure 3 shows the change of MR curves as the illuminated area increased step by step. As the reversed region expanded from the left to the right side as shown in Figure 3, the negative MR peak revealed from the 1-region and its intensity increased. As the illuminated number increase, the positive MR peaks and its fronts become complicated. Particularly, the positive MR shapes of 3 and 5 region have a negative MR ratio at +85 Oe. The distorted MR shape is similar to a 90 degree MR curve. When the external magnetic field is perpendicularly applied to the direction of exchange anisotropy, the MR peak changed to the distorted shape [8]. It could therefore be deduced that the magnetization between the illuminated

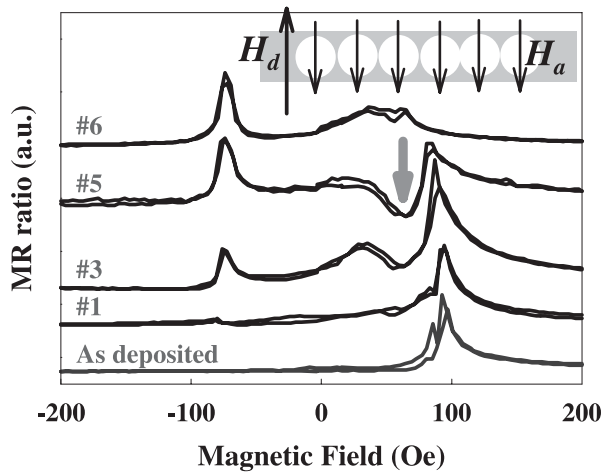

Fig. 3. The change of MR curves of the strip-patterned Ta(5 nm)/NiFe(11 nm)/FeMn(16 nm)/Ta(5 nm) films according to the region of laser annealing expands up to 6, where the laser power is 300 mW.

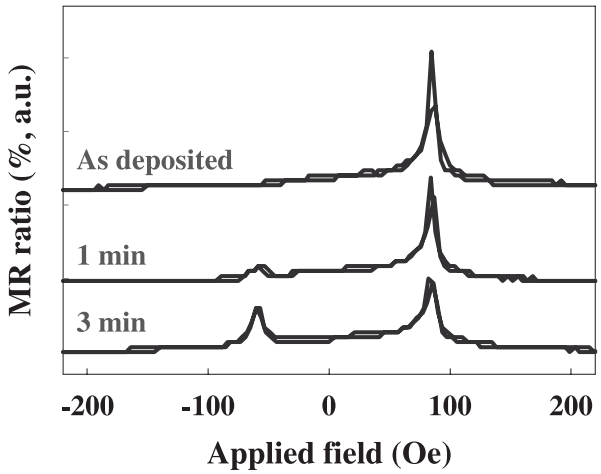

Fig. 5. The change of MR curves as a function of illumination time of laser annealing up to 3 min, where the laser power is 300 mW.

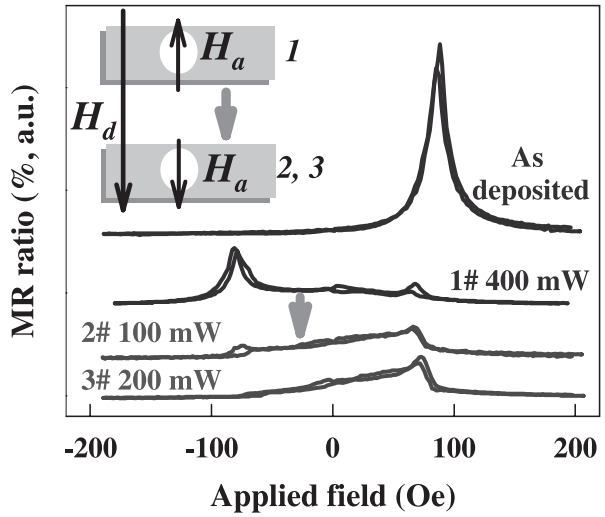

Fig. 4. The change of MR curves of the strip-patterned NiFe(11 nm)/FeMn(16 nm) bilayer for a restored applied field and various laser power.

regions was dispersed from the anisotropy direction, and its direction at the edge of the sample rotated to 90 degree [9]. The Magnetic domain of laser annealed films will be detailed later on. Also we will show the microscopic domain images using MFM in these patterned films.

The change of MR curves of the strip-patterned NiFe(11 nm)/FeMn(16 nm) bilayer for a restored applied field and various laser power is shown in Figure 4. The MR ratio and the $\boldsymbol{H}_{ex}$ of as-deposited bilayer were 0.9% and +87 Oe, respectively. As the power of laser annealing increased, the positive MR peak at +87 Oe was shrunk, and the negative peak was generated at −63 Oe due to local laser annealing. At the 400 mW, the MR peak was almost transferred from positive to negative direction, even if its value was reduced to 50%. The sample 2 and 3 applied the external magnetic field of reversed direction to restore the exchange anisotropy with a laser power. The negative peak shrunk as the power increase, and the positive one grew up again. However, the intensity of the peak did not restore because of Mn diffusion and intermixing between NiFe and FeMn [10]. Therefore, the laser of low power has to be used to reduce the damage induced by laser.

Figure 5 shows the change of MR curves as a function of illumination time up to 3 minute, where the laser power is 300 mW. As the time increases, the negative MR peak grows up and its growth saturated at 3 minute. After 3 minute, the negative peak did not almost change. It means that magnetization reversal is saturated. Figure 6 shows the magnetic domain structure of locally illuminated region by MFM, where the scan size is 100 μm. The size of damage is almost 150 μm, and its magnetization was broken by direct illumination of laser. In the vicinity of the damage region, the complicated domain wall and 180 degree walls were surrounded. In the far region, the domain structure divided into four domains in the center of illuminated region as shown in top sketch of Figure 6. To study more detail domain structure for whole area, we will measure using MOKE in the further work.

4 Conclusion

local magnetization reversal in exchange-biased NiFe/FeMn films was achieved by laser annealing. As the laser power increases, the MR curve with symmetric peaks at the opposite field was obtained due to the local reversal of exchange biasing. The intensity of opposite MR peak increased as the exposed area expanded. The reversed exchange anisotropy can be restored by

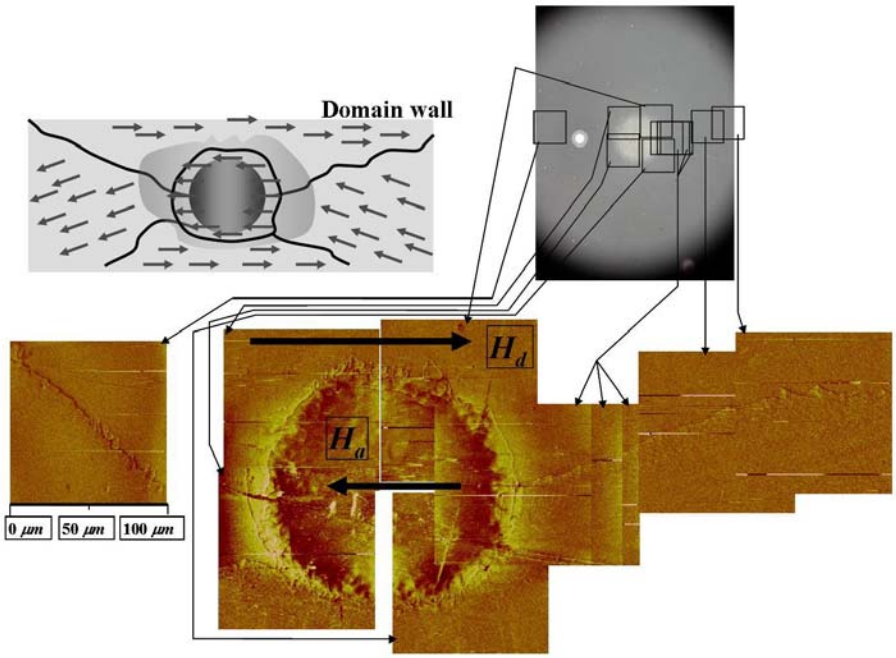

Fig. 6. Magnetic domain structure of locally illuminated region laser measured by MFM where the scan size is 100 μm. The boldic arrow and solid line are magnetic domain direction and boundary, respectivly.

local laser annealing under alternating magnetic field. However, its MR peak was reduced by the damage and interdiffusion. The magnetic domain structure of reversed region were measured. The domain structure divided into four domains from the center of illuminated spot.

This work was supported by Grant No. R05-2003-000-11200-0 from the Basic Research Program of KOSEF and Applied Optics Laboratory of Dankook University.

References

1. S.W. Kim, S.D. Choi, D.H. Jin, K.A. Lee, S.S. Lee, D.G. Hwang, J. Magn. Magn. Mater. **272**, 376 (2004)
2. W.H. Meiklejohn, C.P. Bean, Phys. Rev. **102**, 1413 (1956)
3. G.A. Prinz, Science **282**, 1660 (1998)
4. E.B. Myers, D.C. Ralph, J.A. Katine, R.N. Louie, R.A. Buhrman, Science **285**, 867 (1995)
5. J.Z. Sun, J. Magn. Magn. Mater. **202**, 157 (1999)
6. C. Aroca, I. Tanarro, P. Sanchez, E. Lopez, M. Vazquez, M.C. Sanchez, Phys. Rev. B **42**, 8086 (1990)
7. J.A. Katine, F.J. Albert, R.A. Buhrman, E.B. Myers, D.C. Ralph, Phys. Rev. Lett. **84**, 3149 (2000)
8. C.G. Kim, H.C. Kim, B.S. Park, D.G. Hwang, S.S. Lee, D.Y. Kim, J. Magn. Magn. Mater. **198**, 33 (1999)
9. M.F. Toney, T. Ching, J.K. Howard, J. Appl. Phys. **70**, 6227 (1991)
10. S.W. Kim, J.K. Kim, J.H. Kim, B.K. Kim, J.Y. Lee, J.R. Rhee, S.S. Lee, D.G. Hwang, J. Appl. Phys. **93**, 6602 (2003)